Scientific Research and Essays Vol. 7(23), pp. 2070-2075, 21 June, 2012
Available online at http://www.academicjournals.org/SRE
DOI: 10.5897/SRE11.1977
ISSN 1992-2248 ©2012 Academic Journals

Full Length Research Paper

Fluorescent demonstration of neuronal degeneration in cyanide neurotoxicity through anti protein *G*-colloidal gold conjugate labeling

Ogundele, O. M.

Trinitron Biotech Limited, Science and Technology Complex, Abuja, Nigeria. E-mail: mikealslaw@hotmail.com. Tel: +2347031022702.

Accepted 28 May, 2012

The study of the mechanism of neuronal cell death has been an important aspect of cell biology in the last decade. Considering the somewhat non-specific nature of the methods and the complexity of the neuronal cell cycle, a multi-technique approach has been suggested. This study is aimed at describing a method for demonstration of neuronal degeneration in the visual cortex (molecular layer) of adult wistar rats. It involves the use of colloidal gold (40 nm), conjugated with an antibody against protein G (transmembrane protein) to generate fluorescence; in essence to label the regions of cells with functional membrane, while the region of necrotic cells are empty. This method is complemented by histology to generate overlap images and to detect loss of membrane integrity in neurons at the early stages of progressive neuronal degeneration. An *in vivo* approach was used; 50 mg/Kg BW of potassium cyanide-*Sigma* (KCN) was administered orally to adult Wistar rats to induce neurotoxicity. The animals were sacrificed, and sections were labeled with anti Protein *G*-colloidal gold conjugate. The 40 nm gold particles generated fluorescence in the region of the cells with functional membrane properties, while empty spaces were found in regions of necrotic cells at a magnification of 400× (low magnification).

Key words: Immunoglobin G (IgG), nanoparticles, cell death, bovine serum albumin (BSA).

INTRODUCTION

To describe neuronal degeneration, we must cast our mind first to the concepts governing the ideals of neuronal cell death. In descriptive terms, cell death can be categorized as either apoptotic or necrotic (Katherine et al., 2001). Apoptosis, also called physiological cell death has been characterized first by nuclear changes such that membrane changes occurs later, while necrosis has been characterized more by membrane changes, and nuclear changes, if it occurs, is a late event (Isom et al., 1999; Denison et al., 2009). In cyanogenic neurotoxicity, the mechanism of cell death in the neurons of the *V1 (primary Visual cortex)* has been described more as apoptosis as evident in studies where 20 mg/kg BW and 2 mg/kg BW generated apoptosis (data not shown); while in the entorhinal cortex or dentate gyrus, the mechanism of cell death has been described as necrotic. In both apoptosis and necrosis, membrane changes are paramount, as a similar event is believed to occur at the onset of both modes of cell death.

The ability of cyanide to inhibit Cytochrome C oxidase binuclear centre thus inhibiting the complex V of the electron transport chain is a major event. This leads to accumulation of e^- and subsequent activation of oxygen to generate oxygen radicals or superoxide anions (reactive oxygen species). ROS also reacts with nitrogen to give RNS. The increase levels of ROS results in an increased level of lipid peroxidation. Furthermore, peroxidation of lipid will imply certain level of loss of membrane proteins and lipids, as the lipid bilayer looses it integrity to peroxidation by ROS, the membrane proteins will gradually disengage. A major component of the membranes are the transmembrane proteins *G* which has 3 subunits, and are usually receptors for coordination of neuronal potentials and depolarization of neuronal membrane (α-external sub unit-transmembrane domain, γ-intramembrane domain). This study seeks to use the

fluorescent property of a fluorochrome (colloidal gold), otherwise gold nanoparticles (GNP), in determining the presence of degenerating neurons in sections of the *V1* molecular layer. The particle size employed is 40 nm which can be resolved at a lower magnification fluorescent microscopy or bright field microscopy to reveal the extent of neuronal damage. This technique can also be applied to other specific proteins in degenerating neurons, thus allowing for the localization of a specific neuron and most of its projection.

MATERIALS AND METHODS

All chemical reagents were purchased from Sigma-Aldrich and the IgG from Seradyn Inc. Neurodegeneration was induced by treating the animals with potassium hexacyanoferrate III which was orally administered rather through other means that will bypass the liver, since 90% of cyanide exposure is oral to obtain a sub-lethal dose, capable of generating neurological symptoms in the animal (50 mg/kg BW) based on the LD_{50} for KCN. The treatment duration was 45 days (medium term treatment). The animals were sacrificed at the 45th day by cervical dislocation and the brain tissue was gently excised and fixed in cold 4% paraformaldehyde in PBS (at 4°C). The tissue sections were embedded in 15% gelatin (300 Bloom)/PBS in cryomolds and set at 4°C for one hour. Sectioning was done using a Leica vibrotome, using the method of Andrew P. McMahon Laboratory. 10 μm sections were used, followed by mounting on slides before the labeling with the anti protein-*G*-colloidal gold conjugate.

Preparation of colloidal gold and gold conjugate for immuno gold labelling

1% sodium citrate solution was made by dissolving 1 g of sodium citrate (Sigma) in 100 ml of deionised water (Millipore, France). The water was tested for salts and has a pH of 6.0. Two litres (2000 ml) of the water was placed in a conical flask and 50 ml of 1% gold chloride (99% pure from Sigma; Life Science grade) was added. A stirrer magnet, covered with a tephlon, was inserted into the solution, the hot plate was switched on such that the temperature was set at 70°C, a conical flask 250 ml capacity was inverted to cover opening of the larger conical flask in other to prevent loss of steam by vaporization. The solution was allowed to boil and the stop watch was started, until the colour changes from red to purple (approximately 1 min). 9.6 ml of 1% gold chloride was added and the colour will again change from red to purple, 2 ml 0.7% gold chloride ($AuCl_2$) was then added as the colour was observed to have changed from purple to pink (Wang et al., 2007, 2010; Oliver, 2010; Korosoglou et al., 2006). The solution was allowed to cool by constantly running water on the cone region of the conical flask. The colloidal gold was analyzed using the spectrophotometer in the spectrum region, the peak absorbance recorded (λ_{max}) was 528 nm in a Jenway 5500 spectrophotometer calibrated with distilled water in (650 to 450 nm for colour red solutions). The wavelength of the gold colloid used was measured in a spectrophotometer Jenway 5500 for 40 nm gold (standard λ_{max} between 524 to 528 nm). The particle size as analyzed under the fluorescent microscope was approximately 40 nm ± 1, using the methods of (Liaw et al., 2010; Loesch and Burnstock, 1998).

Preparation of IgG anti protein *G* ()

The antibody was purchased from Seradyn Inc. On arrival, it was gradually thawed, and the salt content was analyzed by adding in an eppendorf tube 90 μl of 0.1 M $AgNO_3$ with 10 μl of the IgG. The salt concentration was high on visual quantification and the antibody was dialyzed in 1 L flask containing 900 ml of 10mM Tris-HCl, pH 8.0 (Ren et al., 2006), the dialysis was done by placing the antibody in a silicon tubing and allowed it to spin overnight. The concentration was determined by using the photometric menu of the spectrophotometer and quartz cuvettes to measure the concentration of the protein at 280 nm. The IgG was then diluted to a final concentration of 0.5 mg/ml (León et al., 2005; Valdivieso et al., 2003). Final desalting was done in a G-25™ Sulphadex column connected to Biorad (Econo UV monitor). The final concentration was then determined by measuring the absorbance in Photometric menu at 280 nm, using a quartz couvette, the final value was determined by dividing the actual value by a protein coefficient of 1.4 (Hsien-Chang et al., 2004; John et al., 2008).

Conjugation of anti protein-*G* to 40 nm gold colloid

The Tris-HCl (pH 8.0) was poured into a beaker and the antibody was added at a concentration of 5 mg/L, the colloidal gold twice the volume of the buffer was the added, and the solution was blocked with 1.5% BSA (Bovine serum albumin, Sigma) added as 10% solution, this is to blick non-specific interactions. 0.05% Sodium azide (Sigma) was added to prevent microbial infection, 1% glycerol was then added to preserve the conjugate. The Solution was centrifuged at 10000 rpm and 4°C, the supernatant was collected and discarded, while the final conjugate was obtained as the sediment from the centrifugation.

Immuno gold labeling

The sections, 10 μm thick, were rinsed in cold 0.1 M phosphate buffer pH 8. This was to normalize the pH of the tissue with that of the incubating solution. The sections were then pretreated with 1% sodium borohydride (Sigma) for 30 min and rinsed in freshly prepared phosphate buffer saline (PBS) three times, at 5 min each to remove the bubbles. The solution was blocked with 1.5% BSA (bovine serum albumin) for 30 min (serum blocking). The slides were incubated with diluted IgG-gold conjugate (1:50) against regular non-specific membrane proteins in the pyramidal cell layer of the primary visual cortex; at room temperature for 3 h. The sections were rinsed in PBS 3 times at 5 min each. Post-fixation was done in 2% glutaraldehyde.

Photomicrography and image retrieval

The slides were examined under the fluorescent mode of Zeiss Primostar with a JVC camera attachment to the third ocular of the microscope, to examine the fluorescence of gold nanoparticles tagged with anti-protein *G* and the locations of the gold conjugate labeled neurons, while regions in the sections with degenerated neurons did not give any fluorescence and were not labeled by the conjugate. The image was retrieved and processed using Image J (NIH recognized image processing software).

RESULTS

The colloidal gold and gold conjugate were gently smeared on a plain glass slide and examined under fluorescence to check for affinity and orientation of the proteins in relation to the ionic properties of colloidal gold.

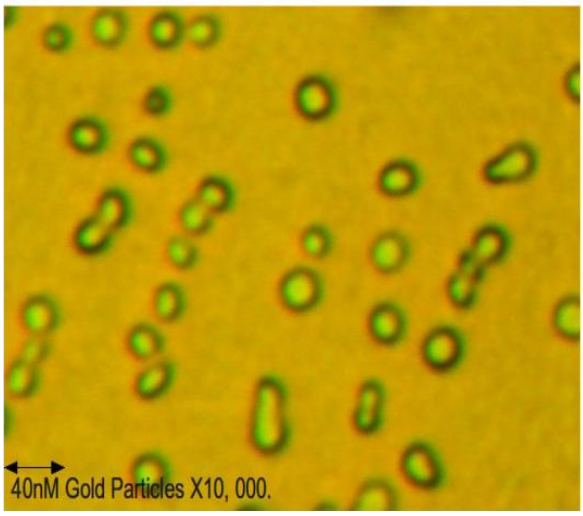

Figure 1. 40 nm colloidal gold under fluorescent microscope, yellowish green fluorescence gold particles under fluorescent microscope (magnification ×5000).

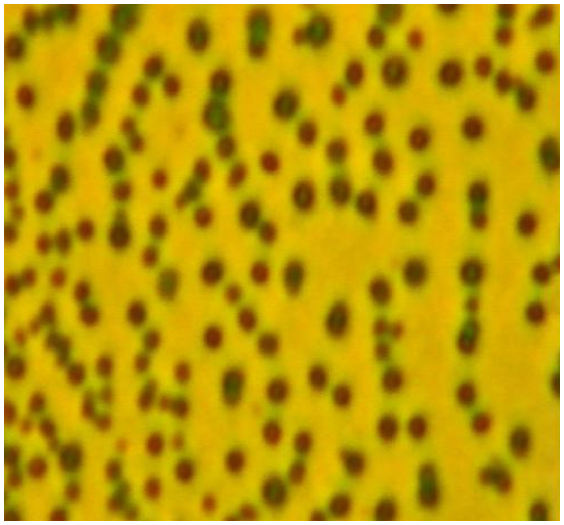

Figure 2. 40 nm colloidal gold under fluorescent microscope. λmax 520 nm microscope model: Zeiss primo star (magnification ×5000).

Observing the light scattering potential of gold colloid as seen in Figure 1, reveals that the outer surface of the colloid gives a yellowish-green fluorescence, compared with the extreme edges with a green fluorescence. Figure 2, which is at a lower magnification, reveals the red fluorescent property of the gold colloid used in this study. Figures 3 reveals the orientation and binding of the IgG-gold conjugate, thus, revealing the binding site between the dark edges of the colloidal gold and the distal part of the Y-shaped IgG molecule (arrow edges) and also illustrated by the schematic diagram of Nagender et al. (2009) (Figure 3).

Neurodegenration of the V1 cortical cells as revealed in 40 nm gold-anti protein-*G* conjugate

The fluorescent view of labeled sections reveals the presence of empty spaces in the section showing the site of degenerated neurons in the molecular cell layer of the visual cortex (Figures 4 and 5). Regions of differential IgG conjugate affinity shows different light scattering and emission property under light microscopy, as seen in Figures 4 and 5. 40 nm particles were used as the procedure was not carried out in cultured cells but rather in vibrotome sections embedded in gelatin. Adjusting the filter and the camera zoom increases the visibility, either by altering the working distance or the contrast of the camera, as described by Sripad et al. (2006) in overcoming the resolution problem, by adopting a stochastic framework and presents a resolution measure that overcomes the limitations of Rayleigh's criterion. This resolution measure predicts that the resolution of optical microscopes is not limited, and that it can be improved by increasing the number of detected photons.

DISCUSSION

Membrane characteristics define necrotic cell death, while nuclei features could be used as structural indicator for apoptosis (Katherine et al., 2001). Neurodegenerative diseases are generally characterized by death of neurons which could either be apoptotic, necrotic or may follow a pattern seen as an apoptotic-necrotic continuum (Pan et al., 2007). The mode of cell death in modeled and *in vitro* experiments has been observed to be dose or intensity dependent, as well as dependant on the cytotoxic pathway adopted by the region of the brain. In *in vivo* studies (Isom et al., 1999; Jerome et al., 2003) involving normal cells, it is expected that anti Protein *G*-conjugate will bid to the external subunit of the target protein which is protein-G. This protein is taken as the target because of its wide distribution on the surface of the neurons, coupled with the loss of the protein in the event of lipid peroxidation in membranes. To describe the loss of Protein *G*-conjugate fluorescent microscopy, we have to give account as to the various events leading to the increase in the level of superoxide anions (ROS) and perhaps lipid peroxidation in cyanide neurotoxicity. Cyanide is potent neurotoxin because of its ability to inhibit Cytochrome *C* oxidase (CcOX) and generate OCN-.

CcOX is an important enzyme of the electron transport chain which is responsible for the transfer of molecular oxygen into water at complex V of the electron transport chain, thus providing the proton gradient required to generate ATP. Cyanide is capable of binding to this

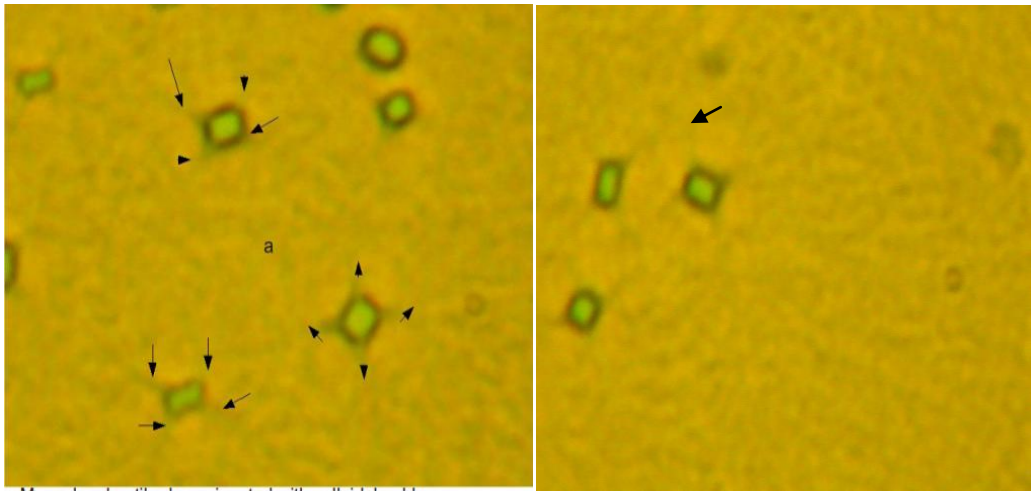

Figure 3. Anti Protein-*G* gold conjugates, showing the orientation of Y-shaped antibodies (arrows) bounded to colloidal gold at direct angles. In most of the particles observed, about 4 antibody units are bounded to a single gold particle (λmax 528 nm) (Magnification X5,000).

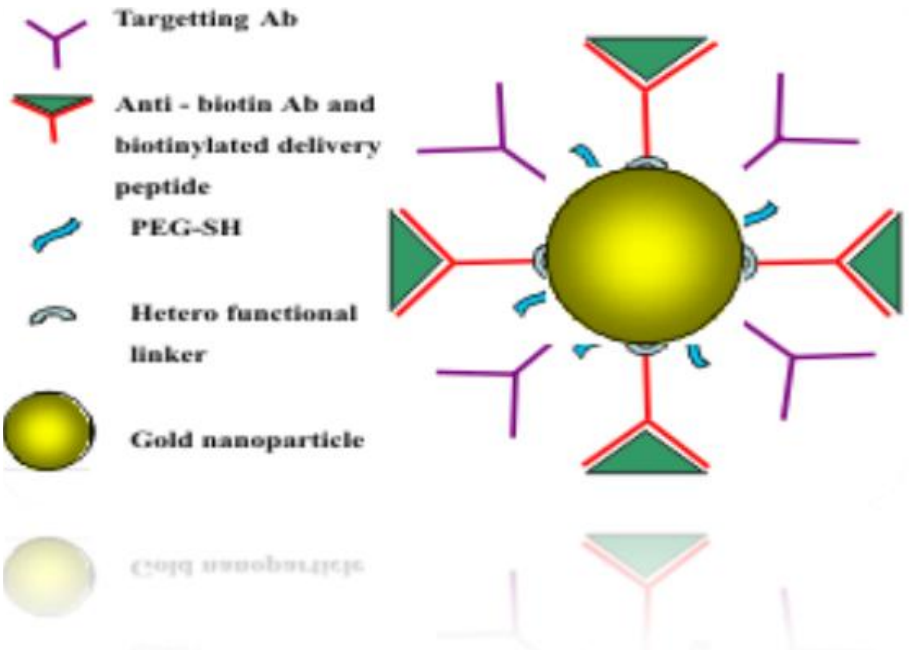

Figure 4. Multifunctional plasmonic nanosensor for imaging intra-cellular biomarker (Nagender et al., 2009)**.** A schematic representation of gold nanoparticle based nanosensor with both targeting and delivery components. Observe the comparison in the 4 winged orientation of conjugates in Figure 3 related to the schematic illustration in Figure 4.

enzyme at its binuclear centre; thus, molecular oxygen is present but not converted into water. The accumulated electrons in the mitochondrial matrix activate the oxygen molecules into O^{3-} which is a ROS. The ROS thus generated leaks back into the cytoplasm, initiating series of reactions including peroxidation of the lipid bilayer of the neuronal membrane (Isom et al., 1999). Peroxidation of lipid will involve loss of membrane proteins, considering the model of a unit membrane as described by Davson and Danielli (1935), the proteins are suspended in the bi-lipid layer. Therefore, it can be derived that a major marker for cell death in the visual

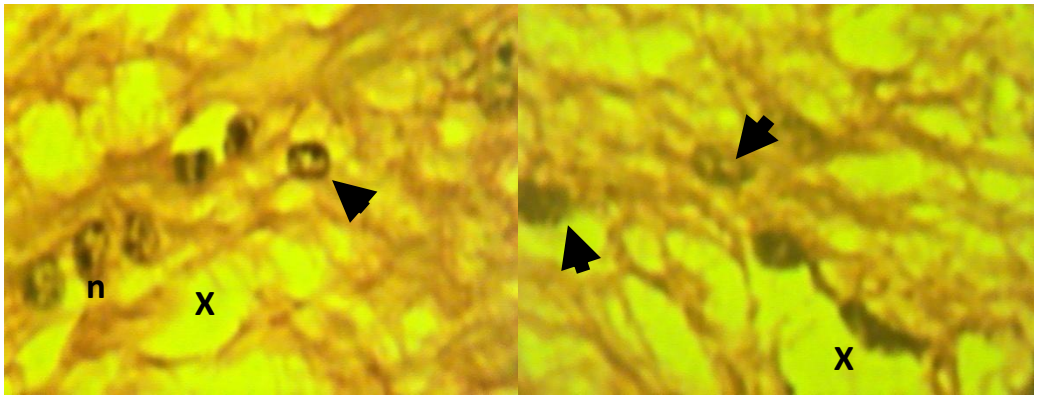

(a) (b)

Figure 5. Fluorescent micrograph of neurons labeled and enhanced fluorescence with colloidal gold (40 nm) conjugated with IgG. Arrow head shows neurons with intact membranes and projections; n indicates intact neuronal membrane. Empty spaces (x) are sites of degenerated neurons with corresponding loss of axonal connection (Magnification ×400).

cortex is loss of transmembrane *G*-proteins. The technique described in this study has both qualitative and quantitative essence, aside from indicating the presence of proteins; it can also be used to quantify the amount of the protein present in the normal neuron. Distribution of membrane proteins can be mapped out by the location of the gold conjugates, while it can be quantified by the chromo aggregation of the conjugates to show regional difference in distribution of the proteins by difference in intensity across the zones of the cortex in microscopy. The interaction between the positively charged spherical surface of the nano particle and the negatively charged aminoacid chain in the tail of the Y-Shaped antibody are pure forms of biological electrostatic reaction. BSA was added to the medium to block non specific proteins from interacting with the gold particle. An evidence of good interaction can be observed in the colour of the gold conjugate before microscopy. The red colour must be retained. If this were not so, the colour will change to purple showing that the gold colloid is now aggregated to form irregularly sized and charged particles that are not capable of binding to antibodies. In diagnostics, purple gold (formulated to contain large particles of over 75 nm) is also possible and can be formulated, but the difference between a formulated purple gold and an aggregated red gold giving purple coloration is the uniformity of the gold colloid. The aggregated gold always have a lighter purple colour and if left for few hours, the aggregated gold will deposit at the bottom of the container leaving a clear top, while a formulated purple gold will remain uniformly suspended in solution. The charged tail was attached to the surface of the gold particle, thus leaving the heavy and light chain forming the limb of the Y shape to be free to interact with the membrane proteins. It is also noteworthy to mention that the limbs (heavy and light chain contains the epitope of the antibodies).

This technique can be applied to study other proteins in normal and degenerating cells and can also be used in low magnification light microscopy. In conclusion, immunogold labeling of protein serves as an important tool for localizing early loss of membrane integrity in degenerating neurons, and also localizing the presence of degenerating and normal neurons in the visual cortex.

In future, immunogold demonstration of neurodegeneration in the substantia nigra, as it concerns Parkinson's disease may be considered.

ACKNOWLEDGEMENT

The author is grateful to Trinitron Biotech LTD, West African Health Organization, and Mr Jonathan Igwe of the Pathology Department, National Hospital, Abuja, Nigeria.

REFERENCES

Davson H, Danielli JF (1935). "A contribution to the theory of permeability of thin films". J. Cell. Comp. Physiol., 5(4): 495.

Hsien-Chang Chang, Ching-Chou Wua, Shinn-Jyh Ding, I-Shiun Linc, I-Wen Sun (2004) Measurement of diffusion and partition coefficients of ferrocyanidein protein-immobilized membranes. Analytica Chimica Acta, 532(2005): 209-214

Isom GE, Gunasekar PG, Borowitz JL (1999). Cyanide and neurodegenerative disease. In: Chemicals and Neurodegenerative Disease (S. C. Bondy, Ed.). Prominent Press, Scottsdale, AZ. pp. 101-129.

Katherine L, Barrett M, Willingham A, Julian Garvin, Mark C. Willingham (2001). Advances in cytochemical apoptosis. J. Histochem. Cytochem., 49: 821-832.

Jerome Niquet, Roger A, Suni G, Denson G, Claude G (2003).Wasterlain Hypoxic neuronal necrosis: Protein synthesis-independent activation of a cell death program. PNAS, 100(5): 2825-2830.

John R, Brent S, John F, Theodore W (2008). Measurement of the second osmotic virial coefficient for protein solutions exhibiting monomer–dimer equilibrium. Anal. Bioch., 377(2): 128-133.

Korosoglou G, Behrens S, Bekeredjian R, Hardt S, Hagenmueller M, Dinjus E, Böhm KJ, Unger E, Katus HA, Kuecherer H (2006). The potential of a new stable ultrasound contrast agent for site-specific targeting. An *in vitro* experiment. Ultrasound Med. Biol., 32(10): 1473-1478.

León G, Lomonte B, Gutiérrez JM (2005). Anticomplementary activity of equine whole IgG antivenoms: comparison of three fractionation protocols. Toxicon, 45(1): 123-128.

Liaw JW, Tsai SW, Chen KL, Hsu FY (2010). Single-photon and two-photon cellular imagings of gold nanorods and dyes. J. Nanosci. Nanotechnol., 10(1):467-73

Loesch A, Burnstock G (1998). Perivascular nerve fibres and endothelial cells of the rat basilar artery: immuno-gold labelling of antigenic sites for type I and type III nitric oxide synthase. <http://www.ncbi.nlm.nih.gov/pubmed/10640179> J. Neurocytol., 27(3):197-204.

Nagender Panyala, Eladia Pena-Mendez, Josef Havel (2009). Gold and nano-gold in medicine: overview, toxicology and perspectives. J. Appl. Biomed., 7(2): 75-79.

Oliver C (2010). Conjugation of colloidal gold to proteins.Methods Mol Biol., 588: 369-373.

Pan Y, Neuss S, Leifert, Fischler M, Wen F, Simon U, Schmid G, Brandau W, Jahnen-Dechent W (2007). Size-Dependent Cytotoxicity of GNPs. Small, 3: 1941-1949.

Ren Q, Liu YJ, Xu B, Han ZB, Lu SH, Ma FX, Chen Z, Han ZC, Xi Bao, Yu Fen, Zi Mian, Yi Xue, Za Zhi (2006). Expression of recombinant human hemangiopoietin and preparation of its polyclonal antibody. Xi Bao Yu Fen Zi Mian Yi Xue Za Zhi, 22(6): 801-803. (Chinese).

Sripad E, Sally Ward, Raimund J (2006). Beyond Rayleigh's criterion: A resolution measure with application to single-molecule microscopy. PNAS, 103(12): 4457-4462.

Denison TA, Koch CF, Shapiro IM, Schwartz Z, Boyan BD (2009). Inorganic phosphate modulates responsiveness to 24,25 (OH)2D3 in chondrogenic ATDC5 cells. J. Cell Biochem., 107(1): 155-62.

Valdivieso E, Bermudez H, Hoebeke J, Noya O, Cesari IM (2003). Immunological similarity between Schistosoma and bovine cathepsin D. Immunol. Lett., 89(1):81-88.

Wang J, Nantz MH, Achilefu S, Kang KA (2010). FRET-like fluorophore-nanoparticle complex for highly specific cancer localization. Adv. Exp. Med. Biol., 662: 407-413.

Wang W, Chen Q, Jiang C, Yang D, Liu X, Xu S (2007).One-step synthesis of biocompatible gold nanoparticles using gallic acid in the presence of poly-(N-vinyl-2-pyrrolidone). Colloid Surface A, 301:73-79.